TRANSACTIONS OF THE CHINESE SOCIETY FOR AGRICULTURAL MACHINERY
Vol. 47, No. 3, 2016

doi:10.6041/j.issn.1000-1298.2016.03.044

Pig Dimension Detection System Based on Depth Image

Li Zhuo Du Xiaodong Mao Taotao Teng Guanghui
(*College of Water Resources and Civil Engineering, China Agricultural University, Beijing* 100083, *China*)

Abstract: For contactless measurement of pig body dimension andimprovement of pig welfare in the real farm, a pig body dimension detection system was developed based on machine vision technology. An algorithm based on depth image was initiated to obtain pig's contour, because color or gray image are easily affected by various light and dirty on pig body. Firstly, two top view images were captured for each pig by using a stereo vision system. Depth image was obtained through stereo image matching. Depth background subtraction algorithm was used to get pig height data, and pig contour was calculated through binary height image. Then a corner extraction algorithm based on concave structure was optimized and simplified to extract four pig head and tail cut points. Then eight pig body dimension measurement key points were calculated, finally five body dimensions including body length, body width, body height, hip width and hip height were detected. Automatic software was developed which combines the algorithm above based on LabVIEW development environment. Three-dimensional detection accuracy of the system was verified by using calibration board in lab, the relative error of detection were less than 1% within 2 m object distance and view center region has the minimum error. Then the system was installed in a commercial farm for verification. 32 Landrace pigs' body dimensions were measured three times manually and then the system snapped pig's image for estimation. Each pig's five body dimensions were detected three times. The result showed the detected values of body dimension had relative error of 2%, and absolute error of less than 2 cm. The pig body detection system based on depth image overcomes the problem of light and dirty on pig, and it can be used to detect pig body dimension contactless in the real pig farm.

Key words: pig; dimension; depth image; contactless; detection

0 Introduction

Pig dimension is an important parameter for evaluating pig growth and is also a key index for breeding and evaluation of meat quality[1]. Body length, body width, body height and chest circumference etc. have positive correlation with body mass, and body dimension could be used to estimate body mass[2-3]. Seasoned farmers can estimate pig mass with only eyes, however this method cannot be rapidly replicated and promoted. Machine vision technology can accurately measure the object shape information without any contacts[4-5]. Animal warfare is improved and animal stress caused by traditional measurement method is avoided[6-10].

A lot researches using machine vision technology to measure animal body dimension and shape have been done. The method of using a single camera from one side to photograph pig height is a direct way. But pigs are easy to keep out with each other[11-12], it can't be used in pig farms. The method with two cameras on both sides is most used for measuring dairy cow body shape which pass a fixed routine[6-7, 13]. MENESATTI et al.[14] developed a portable stereo vision system to detect sheep's hip height, chest depth and body length, however completely manual selection of measurement points has low efficiency. A pig body dimension automatic detection and body estimation system based on stereo vision was developed in our lab[2]. Eleven body dimensions were measured by using pig body measurement points extract algorithm based on concave structure and convex hull analysis. This system has too many body measurement points and lower success rate. Using color or gray image to extract pig contour is hard to adapt various light environment in piggery. The dirt on pig body and highlight object

Received date: 2015-10-10 Accepted date: 2015-11-17
Supported by "Twelfth Five-year" National Key Technology Support Program (Grant No. 2014BAD08B05)
Corresponding author: Teng Guanghui, Professor. E-mail: futon@cau.edu.cn. Tel: +86-13910098265.

on the ground will cause contour extraction error.

Depth image is also named as range image. It records distance information between each point in the view and camera, it can reflect three-dimensional features on object surface. Extract object contour which based on depth image can avoid the problem brought by color close between background and foreground[15]. Kinect is a customer depth camera. It can quickly acquire object depth information. However it has some disadvantages, such as low image resolution and lower precision when object distance is beyond 1m. Most researches use it to study behavior or character[16-18].

Different breeding pigs have discrepancy model for body dimension estimate weight[19]. This article selects Denmark Landrace as a research object. A stereo vision hardware is constructed. An algorithm about detecting pig top view contour is based on depth image. Filter method for body dimension detection points is combined, and a pig body detection system is built on LabVIEW development environment. Detection precision of system is tested in lab, and pig body detection precision is verified in a real farm.

1 System design

1.1 Hardware system of stereo vision detection

Above the pigsty drinkers, two Basler (Germany) acA - 1600 - 20gc cameras were parallelly set up vertical to the ground. Space between two cameras optical axis is 115 mm. CCD size is 7.15 mm × 5.43 mm with a resolution of 1 624 pixels × 1 234 pixels, so the pixel size is 4.4 μm × 4.4 μm. Two Computar (Japan) H0514 - MP lens with 5 mm fixed focal length were used. The cameras were set up 2.5 m above the ground. Due to fattening pig has 70 cm highest body height, the public view in height of the swine is calculated as 2.46 m × 1.95 m, which is larger than an adult pig. A whole pig is covered in one picture. The public view in height of the swine is described as

$$w = \frac{a}{f} z - b \tag{1}$$

Where w is the length of the view, a is the side length of CCD, f is the focal length of camera, z is the object distance, and the baseline b is the distance between two optical centers of two cameras.

1.1.1 3D detection principle of binocular vision

The principle of binocular vision inspection object space coordinates is shown in Fig. 1. Points B and C represent the lens optical center. Point A is a point on pig back. Points E (x_1, y_1) and D (x_2, y_2) are image points of A on two cameras' CCD plane. In an ideal model of binocular vision, two cameras are placed in parallel, their CCD planes are coplanar and row aligned, so $y_1 = y_2$. And d stands for the parallax of two imaging points, calculated as follows

$$d = |x_1 - x_2| \tag{2}$$

Three-dimensional coordinate of pig back point A is calculated as follows

$$x = x_1 \frac{z}{f} \tag{3}$$

$$y = y_1 \frac{z}{f} \tag{4}$$

$$z = \frac{f}{x} d \tag{5}$$

Calculation formula detection accuracy for Δd depth of point A is[20]

$$\Delta z = \frac{z^2}{fb} \Delta d \tag{6}$$

Where Δd represents parallax matching accuracy, typically uses 1/5 of camera pixel size.

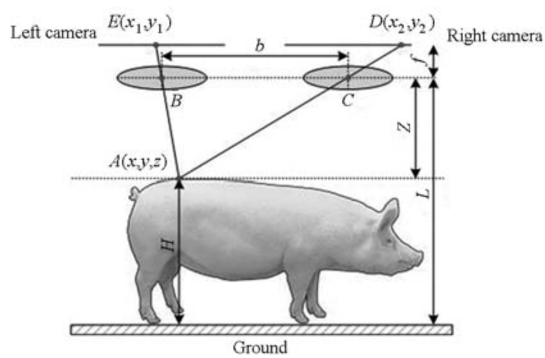

Fig. 1 Principle of binocular vision

Two cameras are spaced about 115 mm, and pigs' height range is 40 ~ 70 cm. Combined with the height of cameras, theoretically pig detection accuracy is 4.96 ~ 6.75 mm. Considering pig measuring stick has a detection accuracy of 0.5 cm, the theoretical detection accuracy of the system is acceptable.

1.1.2 Individual identification of pigs

Each pig wears a radio frequency identification (RFID) electronic tag on its right ear, which meets the ISO11784/11785 international standards of animal frequency identification. A RFID reader was mounted on the right side of drinker. Limited rails are set up in the drinking zone, width only allowed a pig enter at one time to drink. System hardware structure is shown in Fig. 2.

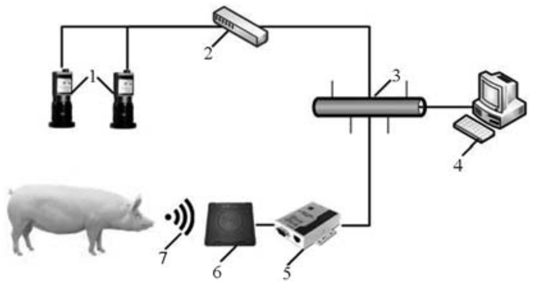

Fig. 2 Hardware architecture of machine vision system

1. Binocular cameras 2. Gigabit LAN switch 3. LAN 4. Main server 5. Transform server for serial port to the network 6. RFID reader 7. RFID ear tag

1.2 Body size detection software

Body dimension detection software is combined with four parts including image automatically capture, depth image calculation, pig outline obtained and body dimension calculations. Automatic image acquisition and dimension detection were developed in LabVIEW graphical development platform and the VDM.

1.2.1 Automatic image capture program

Automatic image acquisition program firstly judged the time, which only captures images in the daytime when pigs have more activities. When the reader detected ear number of the drinking pig, two cameras simultaneous acquire one image. Then whether the captured image has been exposed or underexposed areas is determined. Because the lack of texture pixels will lead to match failure, pixels depth data can't be obtained. First, the entire image is divided into a several areas with 64 pixels × 64 pixels. The statistical proportion of maximum and minimum values in the image region is calculated. If the ratio exceeds a set threshold, then the region is considered as overexposed or underexposed. The threshold value is 0.4 in this study. If all areas are not overexposed or underexposed, then the two images are saved.

1.2.2 Depth image calculation

Flow of body dimension detection software is shown as Fig. 3. Because two cameras can't guarantee completely parallel in actual installation. The left and right images need to be corrected according to system calibration parameters. Left and right image were corrected to standard parallel images. Next step is matching left and right images, which means to find the corresponding projected pixel on the left and right images of the same object. The difference of X coordinate around the two image pixels is called parallax. All points' parallax is called dense parallax images. The maximum and minimum parallax could be determined by combined focal length, camera parameters and the object distance range of binocular vision system. Parallax beyond the range is regard as valid matches. SGBM (Semi-global block match) algorithm proposed by a German scholar Hirchmuller is used in this study. It uses multi-directions of the one-dimensional smooth constraint to approximate a two-dimensional smooth constraint. Result of this algorithm is comparable with graph cut method and the belief propagation method, and the efficiency is much higher than these algorithms. And its implementation process has a relatively regular structure which makes it easily mapped to the parallel processing platform[21-22]. It is conducive to enhance image matching speed in the future.

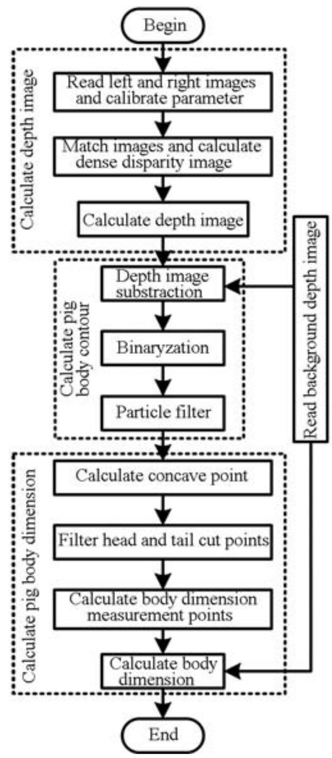

Fig. 3 Flow chart of body detection program

After obtaining a dense disparity image, according to Eq. (3), each pixel's depth data corresponding to left image is calculated. Because there is certain ground water scattering angle, and precision problems of equipment installation, camera's CCD is not always parallel with the ground plane. Single camera height will cause height variation[2]. Therefore, this study first calculate depth data of the ground. Pigs' height information is extracted by subtracting the background depth image from the foreground depth image, which is calculated as

$$H = L - Z \tag{7}$$

1.2.3 Pig contour extraction

Conventional image processing commonly uses grayscale or color image to extract pig contour. In natural lighting piggery, the complex illumination environment, lots of pig dirt and stains on the ground will cause pigs contour extraction errors. Fig. 4a is the grayscale image of pig house. Niblack local threshold binaryzation is used to obtain Fig. 4b. It can be seen the extracted pigs contour is incomplete. The depth image of Fig. 4a is Fig. 5a. The method of using depth image to extract pig contour is insensitive to light and pig's color. The global binary effect of depth image is shown in Fig. 5b, and the binaryzation ranges from 230 to 180.

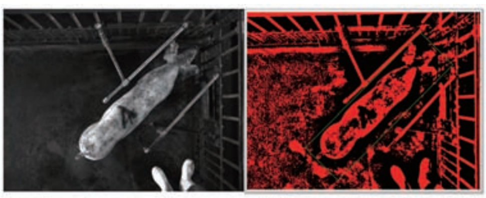

(a) Gray image (b) Binary image

Fig. 4 Gray image binarization

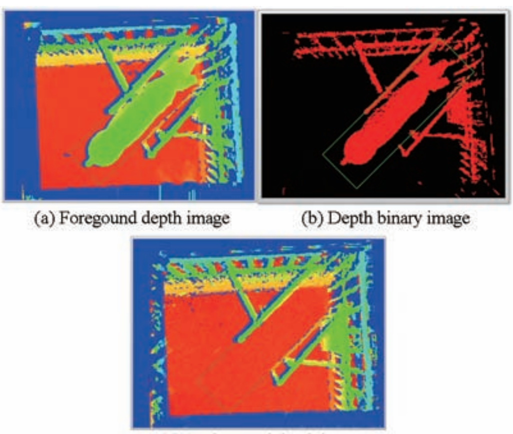

(a) Foregound depth image (b) Depth binary image

(c) Background depth image

Fig. 5 Depth image binarization

In Fig. 5b, it's apparent that the pigs contour extracted from depth image binarization is more complete. And only a part of pixels has close height to the rail was remained. Therefore background subtraction is used firstly, using Fig. 5c minus the foreground depth image Fig. 5a to remove depth data of static background such like limit railings. Then Fig. 6a is obtained. Because pig height general locates 30 ~ 70 cm, good binary image will be obtained using proper threshold to binary Fig. 6a, pig outline has been extracted more completely; however there are some particles that need some morphological operations. After particle filtration, the final pig outline is shown as Fig. 6b.

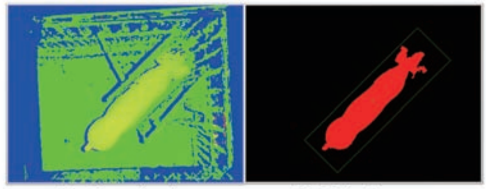

(a) Subtraction image (b) Pig body contour

Fig. 6 Binarization of depth subtraction image

1.2.4 Body dimension detection algorithm

This algorithm based on analysis of convex hull for pig head and tail removing can detect pigtail root and ear dividing points[2, 23]. Pig body dimension detecting key points were calculated as follows:

(1) Calculate the envelope line of pig particle, and calculate coincident points of envelope and contour.

(2) Calculate envelope length between adjacent coincidence points, and envelope segments with length greater than 30 pixels were remained.

(3) Distance d_n between contour point and the envelope line is calculated. The point having maximum distance is selected as an alternative point for tail root and ears split point, and the maximum distance is called depth of the concave (Fig. 7).

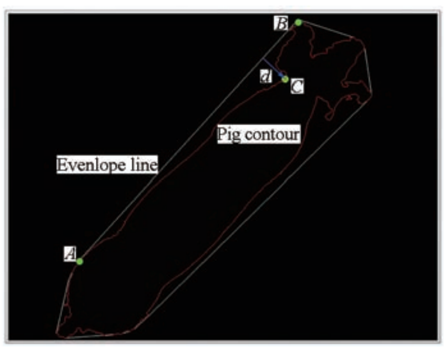

Fig. 7 Diagram of concave structure

(4) As the location of drinker is fixed, the orientation of pig can be easily determined. Using pig particle minor axis (S) as the dividing line, these points were split into ears and tail cut candidate points. Two farthest points from minor axis were selected as tail root split points. Two nearest points from minor axis were selected as head split points.

Above algorithm of step (2) uses a pixel parameter, when the object distance or camera parameters of the system change, the fixed-pixel filter conditions tend to fail. Such as this system have higher camera resolution. The length statistical distribution of the envelope of Fig. 8 is shown in Fig. 9. It could be seen only a few ears and tails split-point have longer envelope segments. If filter condition is envelope segment length greater than 30 pixels, it will result in an excessive number of segments and bring difficulties to the subsequent process. However, if the camera has less pixels, the object distance is larger, or even envelope is shorter, 30 pixel filter conditions may cause leakage of the election. As that can be seen from Fig. 8, there are 10 obvious pig contour corner: 2 on the tail, 2 on abdomen and buttocks junction, 2 on abdomen and shoulder joints, 2 on neck, 2 on head and ears junction. So the scale factor is used as filter in this study, only the 10 longest line segments of envelope were selected.

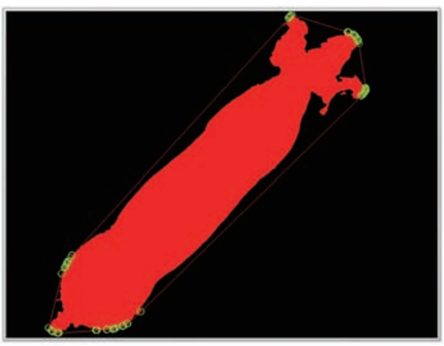

Fig. 8 Coincident points between convex hull and pig contour

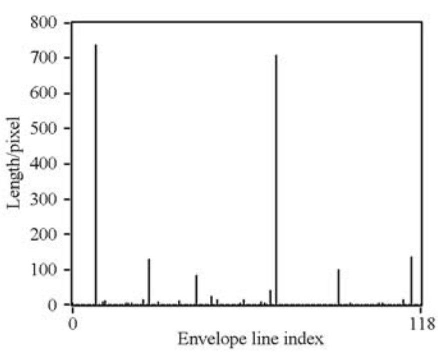

Fig. 9 Length of convex hull line segment

Step (4) of the algorithm uses the farthest corner and the nearest corner to select ears and tail root cut points. When the pig shoulder is wider, the envelope will coincide with contour in the shoulder, which may lead to corners of the shoulder and abdomen are chosen by mistake. To solve this problem, this study proposes a parameter, called the normalization factor of corner for pig body proportion (NFCPBP), which is calculated by distance of corner away from the minor axis divide half pig particle length (l), as shown in Fig. 10.

$$R = \frac{2d_n}{l} \tag{8}$$

Due to most fattening pigs need to cut the tail, the scope of activities pig tail is smaller. The tail length represents a smaller proportion of the total length of the body. After testing multiple images, the NFCPBP of pig tail root generally lies between 0.43 and 0.5, and pig head activities is large, so the neck split point coefficient R is generally between 0.25 to 0.4.

Fig. 10 Corners of pig body contour

After the above filter processing, the extraction pig head and tail split points are shown in Fig. 11. Only five dimensions which are easy to manually verify were examined in this study. Body dimension measuring point extraction schematic diagram is shown in Fig. 12. Firstly, the midpoint of ears split points 1 and 2 is determined as point 5, and point 12 is midpoint of tail split points 3 and 4. Pig body length is from point 5 to point 12. From points 1 or 2, along the major axis direction of pig particles, rectangle a_1 is determined after 1/12 to 1/3 of body length. The maximum width of contour within the rectangular a_1 is pig shoulder width. From points 3 and 4, rectangle b_1 is determined forward 1/12 to 1/3 body length distances. The maximum width of pig contour inside rectangular b_1 is hip width. The midpoint of two measurement points for body wide is body height measurement point; the

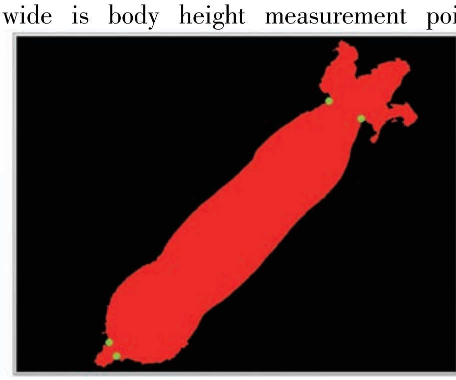

Fig. 11 Cut points of pig head and tail

midpoint of two hip width measurement points is the hip height measurement point. Formulas for calculating each body size are shown in Tab. 1.

Fig. 12 Automatic detection of body measurements key points

1,2. Ear cut points 3,4. Tail root split points 5. Midpoint of neck 6,7. Measuring points for shoulder 8. Measuring points for body height 9,10. Measuring points for hip width 11. Measuring points for hip height 12. Midpoint of tail root

Tab. 1 Equation of body size measurement

Dimension	Measurement point	Description	Formula
Body length	5,12	Horizontal distance	$\sqrt{(x_5-x_{12})^2+(y_5-y_{12})^2}$
Body width	6,7	Horizontal distance	$\sqrt{(x_6-x_7)^2+(y_6-y_7)^2}$
Body height	8,B8 *	Vertical distance	$z_{B8}-z_8$
Hip width	9,10	Horizontal distance	$\sqrt{(x_9-x_{10})^2+(y_9-y_{10})^2}$
Height	11,B11	Vertical distance	$z_{B11}-z_{11}$

* B means point on background image.

1.3 Verification of the system accuracy

1.3.1 Verification system detection accuracy

To verify the accuracy of the detection system, calibration plate was used in the lab to carry out X, Y, Z axis detection accuracy verification at different distances and different regions. Standard detection object is a calibration plate with a 10 × 7 matrix of dots, and the circle center spacing is 4 cm. Detected objects is Z-axis height and X、Y axis space of circle center. Distance from camera to the ground is about 192 cm.

Calibration board images were collected at 15 different heights with range of 0 ~ 80 cm. Four edge heights of calibration plate were manual measured and averaged. About three pairs images were taken to calculate depth images, X, Y, Z coordinates of dot center and X-axis, Y-axis spacing of dot center. Distances between calibration plate point and ground were extracted through subtract Z-axis distance from ground depth. All distances were averaged.

The whole view is divided into five regions, which are upper left, lower left, upper right, lower right and center. The calibration board images were acquired at 150 cm away from camera in each region, and the calculated content is same as above. Three images' data were averaged in each region.

1.3.2 Measurement accuracy verification of pig dimension

In 9th fattening house of Tianjin Huikang pig breeding Ltd., there are 16 Landrace finishing pig were selected in piggery 6. Pigs are 141 ~ 149 d old. In June 25 and July 2 of 2014, pigs' body dimension data were measured using a measure tape including body length, body width, body height, hip width and hip height with 0.1 cm accuracy. Because pig will in a state of stress if it is kept in weighing cage, to ensure accuracy of the measured data, the pig dimension should be measured in a free state. When pig is drinking or feeding and its body is in a stable and straight state, the body dimensions were measured. The influence of pig body data from different poses is avoided[24]. Each body dimension was measured three times for average. Each body dimension measurement position is shown in Tab. 2.

Tab. 2 Key points of body measurement

Body dimension	Start and end point
Body length	From midpoint of ear root to tail root midpoint
Body width	Twowidest points of shoulder
Body height	Height of body width
Hip width	Twowidest points of hip
Hip height	Height of hip height

Pig images which have better depth quality and pig body is straight without bending were manual selected from each day pig images. Using body dimension automatic measurement program, five body dimensions were detected through average three images' result.

2 System verification and result analysis

2.1 Detection accuracy results of calibration plate

Detection precision of X, Y, Z axes at different distance is shown in Fig. 13. Z-axis relative error decreases as the object distance decreasing. It basically satisfies the relation between detection accuracy and object distance described by detection accuracy calculation Eq. (6). Mean relative error of X axis and Y axis detection are both 0.65%. The maximum relative error distance is 0.84% at 157 cm distance, and the minimum relative error is 0.52% at 120 cm. The average relative error of detection at Z-axis is 0.34%, and the minimum relative error is 0.09% at 136 cm, the maximum relative error is 0.72% at 146 cm. The system achieves high detection accuracy. X axis and Y axis detection accuracy have similar detection errors. Z axis error is generally smaller than those from the X axis and Y axis.

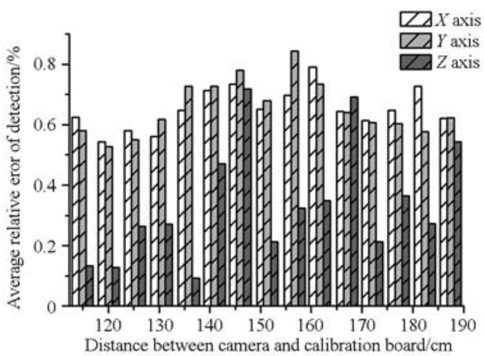

Fig. 13 Detection precision at different heights

The detection accuracy of different regions is shown in Fig. 14. It shows that the central field of camera view has higher detection accuracy, which is consistent with the lens distortion influence. Therefore pig should be placed in a central location of view field when installing cameras, and the distance between camera and pig should as little as possible, in order to improve detection accuracy.

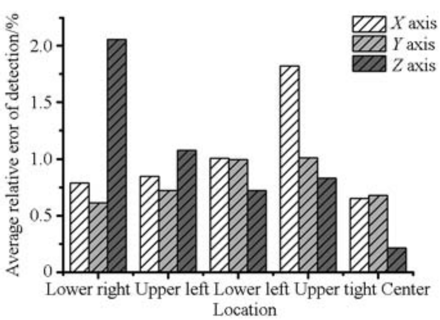

Fig. 14 Detection precision at different areas

2.2 Accuracy results of pigs dimension measure

Image detection error of 32 groups' body dimension on June 25 and July 2, 2014 are shown in Fig. 15. The average absolute errors of all body dimensions are less than 1.5 cm, and most body measurements have errors less than 3 cm. Only parts of the body length and height hip have high errors. The average detection error of 5 dimensions is less than 2 cm. As shown in Tab. 3, body width and hip width detection errors are less than 1 cm, but because of smaller magnitudes, body width and hip width relative errors were 3.05% and 2.25% respectively.

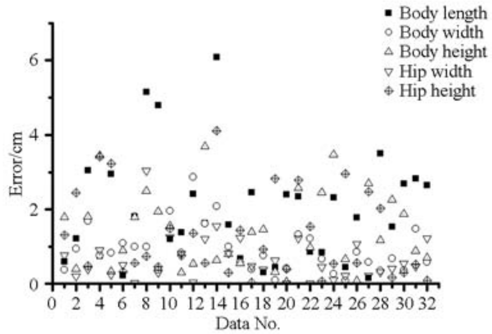

Fig. 15 Error of body size detection

Tab. 3 Average error of body size detection

Body dimension	Absolute error/cm	Relative error/%
Body length	1.97 ± 1.45	1.89 ± 1.37
Body width	0.91 ± 0.62	3.05 ± 2.11
Body height	1.43 ± 1.03	2.58 ± 1.92
Hip width	0.66 ± 0.61	2.25 ± 2.04
Hip height	1.28 ± 1.15	2.09 ± 1.92

2.3 Discussion

It can be seen from Tab. 3 that body width's absolute error is higher than the hip width's, and body height has higher absolute error than hip height. It mainly due to the activities of pig's head is larger and easily affecting body width and body height measurement. In this study, although relatively flat pig images were selected, but because pigs like to play water when drinking and frequently change posture, it results in body width and body height measurement errors. It is recommended that a large number of images during a day are collected and their results are averaged to get more accurate body dimension data.

In addition, as pig has restless nature, it is difficult to ensure pig remains stationary and stays standard posture when snapping a photo or measuring body dimension. Farmers do not need to detect pigs feet every moment. The detection frequency of once a day can meet the requirements. For reducing body mass estimation error, automated program should be developed for strict filtering estimated images to eliminate the gross error, so a more accurate body dimension can be extracted.

3 Conclusions

(1) Method using background depth image subtraction to extract pig contour was proposed, it is proved insensitive to light and dirt on pigs' back during farm experiment test.

(2) Key point of body dimension detection algorithm based on concave analysis was improved. Relative proportion replaces pixel parameter to filter envelope line. Using pig body proportion normalization coefficient of corner points to filter head and tail cut points, and system availability and stability were improved.

(3) Laboratory tests showed that three-dimensional detection relative error of system was less than 1% within 2 m object distance. A test of 32 groups of 16 pigs in farm showed about 2% average relative error of body dimension detection. All body size average detection errors were less than 2 cm, the system can accurately detect pig body dimensions.

References

[1] DOESCHL-WILSON A B, GREEN D M, FISHER A V, et al. The relationship between body dimensions of living pigs and their carcass composition[J]. Meat Science, 2005, 70(2): 229-240.

[2] FU Weisen. Study of pig's body dimensions detection and weight estimation based-on binocular stereovision [D]. Beijing: China Agricultural University, 2011. (in Chinese)

[3] YANG Yan. Study on the estimation of pig's dimensions and weight based on computer vision techniques[D]. Beijing: China Agricultural University, 2006. (in Chinese)

[4] GUO Hao. Study on 3D data capturing and processing methods for live animal[D]. Beijing: China Agricultural University, 2015. (in Chinese)

[5] GUO Hao, MA Qin, ZHANG Shengli, et al. Prototype system of shape measurements of animal based on 3D reconstruction[J]. Transactions of the Chinese Society for Agricultural Machinery, 2014, 45(5): 227-232. (in Chinese)

[6] TASDEMIR Sakir, URKMEZ Abdullah, INAL Seref. Determination of body measurements on the Holstein cows using digital image analysis and estimation of live weight with regression analysis[J]. Computers and Electronics in Agriculture, 2011, 76(2): 189-197.

[7] TASDEMIR Sakir, URKMEZ Abdullah, Inal Seref. A fuzzy rule-based system for predicting the live weight of Holstein cows whose body dimensions were determined by image analysis [J]. Turkish Journal of Electrical Engineering and Computer Sciences, 2011, 19(4): 689-703.

[8] OCHOA Zaragoza Luis Enrique. Evaluation of the accuracy of simple body measurements for live weight prediction in growing-finishing pigs[D]. Champaign: University of Illinois at Urbana-Champaign, 2010.

[9] ENEVOLDSEN Carsten, KRISTENSEN Troels. Estimation of body weight from body size measurements and body condition scores in dairy cows[J]. Journal of Dairy Science, 1997, 80(9): 1988-1995.

[10] BRANDL Nabil, JØRGENSEN Erik. Determination of live weight of pigs from dimensions measured using image analysis [J]. Computers and Electronics in Agriculture, 1996, 15(1): 57-72.

[11] YANG Yan, TENG Guanghui, LI Baoming, et al. Measurement of pig weight based on computer vision [J]. Transactions of the CSAE, 2006, 22(2): 127-131. (in Chinese)

[12] FU Weisen, TENG Guanghui, YANG Yan. Research on three-dimensional model of pig's weight estimating[J]. Transactions of the CSAE, 2006, 22(14): 84-87. (in Chinese)

[13] VIAZZI S, BAHR C, VAN HERTEM T, et al. Comparison of a three-dimensional and two-dimensional camera system for automated measurement of back posture in dairy cows[J]. Computers and Electronics in Agriculture, 2014, 100(1): 139-147.

[14] MENESATTI Paolo, COSTA Corrado, ANTONUCCI Francesca, et al. A low-cost stereovision system to estimate size and weight of live sheep[J]. Computers and Electronics in Agriculture, 2014, 103(4): 33-38.

[15] WU Xin, WANG Guiying, CONG Yang. Object recognition method by combining color and depth information[J]. Transactions of the CSAE, 2013, 29(25): 96-100. (in Chinese)

[16] KONGSRO Jørgen. Estimation of pig weight using a Microsoft Kinect prototype imaging system [J]. Computers and Electronics in Agriculture, 2014, 109(11): 32-35.

[17] GUO Hao, WANG Peng, MA Qin, et al. Acquisition of appraisal traits for dairy cow based on depth image[J]. Transactions of the Chinese Society for Agricultural Machinery, 2013, 44(Supp. 1): 273-276. (in Chinese)

[18] LIU Bo, ZHU Weixing, YANG Jianjun, et al. Extracting of pig gait frequency feature based on depth image and pig skeleton endpoints analysis [J].

Transactions of the CSAE, 2014, 30(10): 131 – 137. (in Chinese)

[19] LI Zhuo, MAO Taotao, LIU Tonghai, et al. Comparison and optimization of pig mass estimation models based on machine vision[J]. Transactions of the CSAE, 2015, 21(2): 155 – 161. (in Chinese)

[20] BRADSKI G, KAEHLER A. Learning OpenCV: computer vision with the OpenCV library [M]. Sebastopol, CA: O'Reilly Media Inc, 2008: 442.

[21] LIU Zhaohua, YANG Yuxia, MA Daxi, et al. Study on semi-global matching algorithm extended for multi baseline matching and parallel processing method based on GPU[J]. Science of Surveying and Mapping, 2014, 39(11): 99 – 103. (in Chinese)

[22] HIRSCHMULLER Heiko. Stereo processing by semiglobal matching and mutual information[J]. IEEE Transactions on Pattern Analysis and Machine Intelligence, 2008, 30(2): 328 – 341.

[23] LIU Tonghai, TENG Guanghui, FU Weisen, et al. Extraction algorithms and applications of pig body size measurement points based on computer vision [J]. Transactions of the CASE, 2013, 29(2): 161 – 168. (in Chinese)

[24] LI Zhuo, LUO Cheng, TENG Guanghui, et al. Estimation of pig weight by machine vision: a review [C] // Computer and Computing Technologies in Agriculture, 2013,2:42 – 49.

doi:10.6041/j.issn.1000-1298.2016.03.044

基于深度图像的猪体尺检测系统

李　卓　杜晓冬　毛涛涛　滕光辉

(中国农业大学水利与土木工程学院, 北京 100083)

摘要: 为实现生猪饲养过程中体尺无接触检测,设计了一套基于双目视觉原理的猪体尺检测系统。针对色彩图像提取猪体轮廓易受污物和光照干扰的问题,提出基于深度图像的猪体轮廓提取算法。使用双目视觉系统获得猪体深度图像,利用帧差法提取猪只高度信息,并基于高度信息二值化图像,获得猪体轮廓;结合优化的基于凹陷结构的拐点提取算法,筛选体尺检测关键点,计算体长、体宽、体高、臀宽、臀高 5 个体尺,编写了基于以上算法的猪体尺检测程序。双目视觉系统三维检测的实验室验证表明:在 2 m 物距范围内,系统三维检测相对误差均小于 1%;系统在实际猪场对 32 组猪体尺检测结果表明:与手工测量猪体尺相比,本系统检测的体尺平均相对误差在 2% 左右,平均误差小于 2 cm。试验证明基于深度图像的猪体尺检测系统不容易受到脏污和光照干扰,能够实现生猪饲养过程中猪体尺的无接触检测。

关键词: 猪; 体尺; 深度图像; 无接触; 检测

中图分类号: TP391; S818　　**文献标识码**: A　　**文章编号**: 1000-1298(2016)03-0311-08

Pig Dimension Detection System Based on Depth Image

Li Zhuo　Du Xiaodong　Mao Taotao　Teng Guanghui

(*College of Water Resources and Civil Engineering*, *China Agricultural University*, *Beijing* 100083, *China*)

Abstract: For contactless measurement of pig body dimension andimprovement of pig welfare in the real farm, a pig body dimension detection system was developed based on machine vision technology. An algorithm based on depth image was initiated to obtain pig's contour, because color or gray image are easily affected by various light and dirty on pig body. Firstly, two top view images were captured for each pig by using a stereo vision system. Depth image was obtained through stereo image matching. Depth background subtraction algorithm was used to get pig height data, and pig contour was calculated through binary height image. Then a corner extraction algorithm based on concave structure was optimized and simplified to extract four pig head and tail cut points. Then eight pig body dimension measurement key points were calculated, finally five body dimensions including body length, body width, body height, hip width and hip height were detected. Automatic software was developed which combines the algorithm above based on LabVIEW development environment. Three-dimensional detection accuracy of the system was verified by using calibration board in lab, the relative error of detection were less than 1% within 2 m object distance and view center region has the minimum error. Then the system was installed in a commercial farm for verification. 32 Landrace pigs' body dimensions were measured three times manually and then the system snapped pig`s image for estimation. Each pig`s five body dimensions were detected three times. The result showed the detected values of body dimension had relative error of 2%, and absolute error of less than 2 cm. The pig body detection system based on depth image overcomes the problem of light and dirty on pig, and it can be used to detect pig body dimension contactless in the real pig farm.

Key words: pig; dimension; depth image; contactless; detection

收稿日期: 2015-10-10　修回日期: 2015-11-17

基金项目: "十二五"国家科技支撑计划项目(2014BAD08B05)

作者简介: 李卓(1987—),男,博士生,主要从事机器视觉与测控技术在设施农业中的应用研究,E-mail: lizhuo_lin@163.com

通信作者: 滕光辉(1963—),男,教授,博士生导师,主要从事农业生物环境智能控制和数字畜牧研究,E-mail: futong@cau.edu.cn

引言

猪的体尺是评价猪生长的重要参数,也是种猪选育和肉质评价的重要指标[1]。猪只体长、体宽、体高、胸围等三维体尺与体质量呈正相关,可用体尺估测体质量[2-3]。有经验的养殖人员虽然也能够通过目测体尺估测体质量,但这种方法无法快速复制和推广。机器视觉技术可以无接触、准确地测量物体外形和表征信息[4-5],避免传统测量方法导致动物应激[6-10],提高动物福利。

目前使用机器视觉技术测量动物的体尺和性状已有较多研究。单个相机侧面拍照获取猪体高度的方法较为直接,但猪只间容易相互遮挡[11-12],难以应用于猪场;侧面放置相机的方法多数应用于测量经过固定线路的奶牛体型[6-7,13]。MENESATTI 等[14]开发了一套便携式立体视觉系统检测羊的臀高、胸深、体长,但全靠手工选择体尺测点的方法效率较低。本实验室开发的一套基于双目视觉技术的猪体尺自动检测与体质量估测系统[2],利用基于凹陷结构和凸包分析的猪体尺测点提取算法,实现 11 个体尺的测量,该系统检测体尺数量多,但检测算法提取成功率不高。利用色彩或灰度图像提取猪体轮廓,难以适应猪舍多变的光照环境,猪身上的脏污和地面高光物体会造成轮廓提取错误。

深度图像(Depth image)也称距离图像(Range image),记录场景中各点与相机间的距离信息,反映物体表面的三维特征,基于深度图像提取物体轮廓可有效区分图像前景和背景,避免因背景和前景颜色接近造成的轮廓提取错误问题[15]。消费级的深度相机 Kinect 解决了快速获取物体深度信息的难题,但仍存在较大缺陷,即深度图像分辨率较低,且超过 1 m 后检测精度差,多用于行为分析或性状评价[16-18]。

不同品种猪只体尺估测体重模型有差异[19],本文选取丹系长白猪为研究对象,搭建一套双目视觉硬件,提出基于深度图像检测猪只俯视轮廓的算法,结合优化的体尺检测关键点筛选方法,在 LabVIEW 平台上开发猪体尺检测系统。在实验室条件下标定系统的检测精度,并在实际猪场开展猪体尺检测精度验证试验。

1　系统设计

1.1　双目视觉检测系统硬件

在猪圈饮水器上方,垂直地面平行架设 2 台 Basler(德国)acA－1600－20gc 型相机,2 台相机光轴间距为 115 mm,CCD 尺寸为 7.15 mm×5.43 mm,分辨率为 1 624 像素×1 234 像素,像素尺寸为 4.4 μm×4.4 μm。镜头型号为 Computar(日本)H0514－MP,固定焦距 5 mm。相机架设在距离地面约 2.5 m 的位置。育肥猪最高体尺为 70 cm 左右,在猪体高度根据

$$w=\frac{a}{f}z-b \tag{1}$$

式中　w——视野长度

a——CCD 边长

f——相机焦距　　z——物距

b——2 台相机光心的距离

计算公共视野范围为 2.46 m×1.95 m,可知其大于一头成年育肥猪的体型,满足猪体图像获取需求。

1.1.1　双目视觉三维检测原理

双目视觉检测物体空间坐标原理如图 1 所示。B 和 C 点为镜头光心,$E(x_1,y_1)$ 和 $D(x_2,y_2)$ 分别为猪体背部点 A 在左右相机 CCD 平面的成像点,在理想双目视觉模型中,2 台相机平行放置,CCD 平面共面且行对齐,所以 $y_1=y_2$。d 为 2 个成像点的视差,计算公式为

$$d=|x_1-x_2| \tag{2}$$

猪体背部点 A 的三维坐标$(x,\ y,\ z)$计算公式为

$$x=x_1\frac{z}{f} \tag{3}$$

$$y=y_1\frac{z}{f} \tag{4}$$

$$z=\frac{f}{x}d \tag{5}$$

A 点深度的检测精度 Δd 的计算公式为[20]

$$\Delta z=\frac{z^2}{fb}\Delta d \tag{6}$$

式中　Δd——视差匹配精度,通常取相机像素大小的 1/5

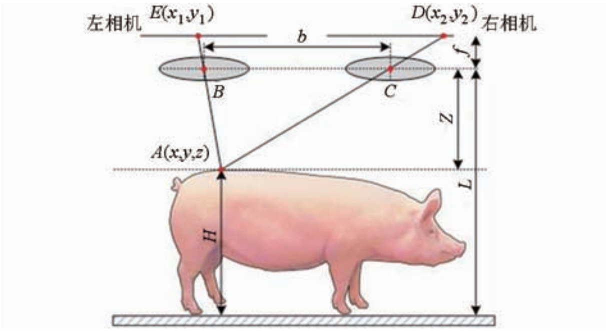

图 1　双目视觉原理

Fig. 1　Principle of binocular vision

2 台相机间距约 115 mm,猪体高度范围为 40～70 cm,结合相机高度,理论猪体检测精度为 4.96～6.75 mm。考虑猪体尺专用测杖的检测精度为 0.5 cm,系统的理论检测精度可接受。

1.1.2　猪只个体识别

每头猪右耳佩戴无线射频电子耳标（Radio frequency identification devices，RFID），满足国际标准 ISO 11784/11785《动物的射频识别》，读卡器安装在饮水器右侧，饮水区设置限位栏杆，宽度仅允许一次一头猪进入饮水。系统硬件结构如图 2 所示。

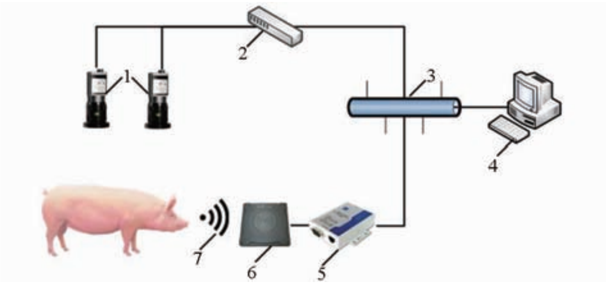

图 2　机器视觉系统硬件结构

Fig. 2　Hardware architecture of machine vision system

1. 双目相机　2. 千兆交换机　3. 局域网　4. 服务器　5. 串口转网络服务器　6. RFID 读卡器　7. RFID 耳标

1.2　体尺检测软件

体尺检测软件由图像自动采集、深度图像计算、猪体轮廓获取和计算猪只体尺 4 部分构成。利用实验室虚拟仪器工程平台（Laboratory virtual instrumentation engineering workbench，LabVIEW）、图形化开发平台和视觉开发模块（Vision development module，VDM）开发图像自动采集程序和体尺检测程序。

1.2.1　图像自动采集

图像自动采集程序首先判断时间，仅在白天猪活动较多时采集图像。当猪只饮水时读卡器检测到猪耳号，左右相机同时采集一张图像，然后判断采集的图像是否有过曝或欠曝区域，因为缺乏纹理的像素会匹配失败，不能够获得像素的深度数据。首先将整张图像分成若干个 64 像素 ×64 像素的区域，统计一个区域图像内的像素最高值和最低值比例，若比例超过设定阈值，则认为该区域过曝或欠曝。本研究中设置判断阈值为 0.4。如果所有区域都没有曝光过度或欠曝，则保存图像。

1.2.2　深度图像计算

体尺检测软件流程如图 3 所示。由于实际安装两台相机无法保证完全平行，需要根据系统标定参数对左右图像进行校正，将左右图像校正为标准的平行图像。之后匹配左右图像，即找到同一物体投影在左右图像上对应的像素点，左右图像像素点 X 坐标之差称为视差，计算所有点的视差得到稠密视差图像。根据双目视觉系统的焦距、相机参数和目标物距范围，确定最大和最小视差，超过该范围的视

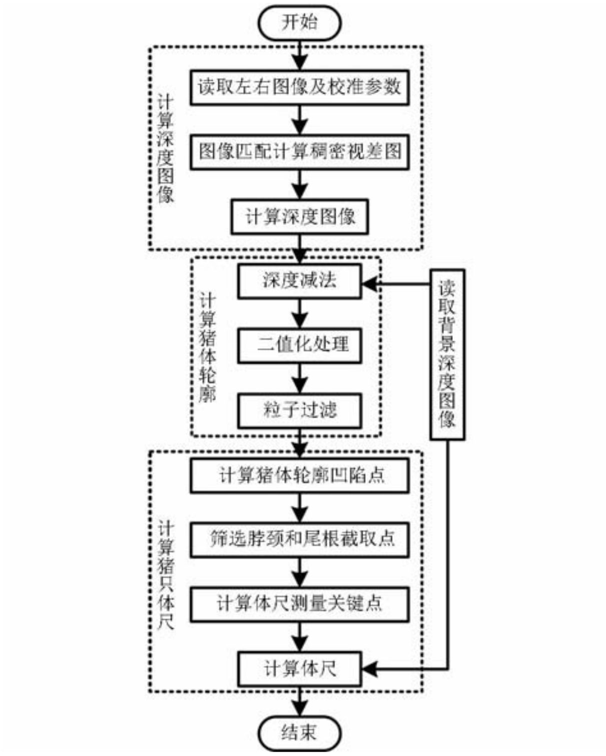

图 3　体尺检测程序流程图

Fig. 3　Flow chart of body size detection program

差认为是无效匹配。本研究采用德国学者 Hirchmuller 提出的半全局块匹配算法 SGBM（Semi-global block match），它通过多个方向的一维平滑约束来近似一个二维平滑约束，不仅可获得与图割法、置信传播法相媲美的处理结果，且执行效率远高于这些算法，同时其实现过程具有比较规则的结构，能够非常容易地映射到并行处理平台[21-22]，有利于提升随后的图像匹配速度。

获得稠密视差图像后，根据式（3）计算左图像的每个像素对应的深度数据。由于地面存在一定散水角度，以及设备的安装精度问题，相机 CCD 平面与地面不一定平行，前人使用单一相机高度将导致高度偏差[2]。故本研究首先计算地面背景的深度数据，通过背景深度图像减去前景的深度图像计算猪体的高度信息，计算公式为

$$H = L - Z \tag{7}$$

1.2.3　猪体轮廓获取

常规图像处理一般采用灰度或彩色图像提取猪只轮廓，但自然照明猪舍中光照环境复杂，且猪体脏污和地面水渍都会造成猪只轮廓提取不准确。对灰度图像（图 4a）使用 Niblack 局部阈值二值化的方法，得到图 4b，可以看出猪体轮廓提取不完整。图 4a 得到的深度图像如图 5a 所示，利用深度图像的猪只轮廓的方法提取对光照和猪体颜色不敏感，深度图像全局二值化效果如图 5b 所示，二值化范围为 230 ~ 180。

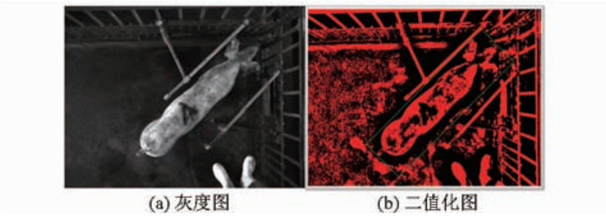

图 4　灰度图像二值化

Fig. 4　Gray image binarization

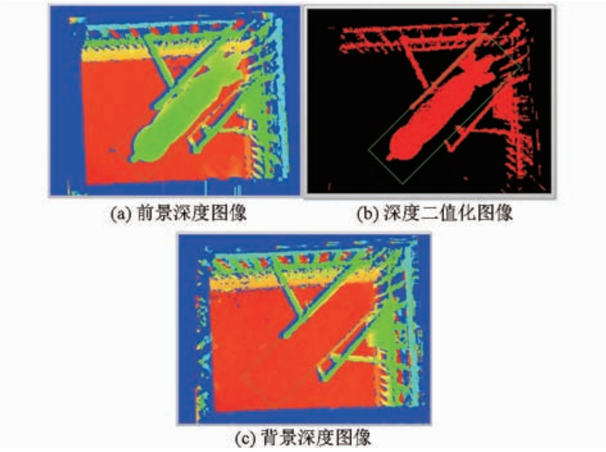

图 5　深度图像二值化

Fig. 5　Depth image binarization

由图 5b 明显看出，深度图像二值化提取的猪体轮廓较完整，只有部分高度与猪体较接近的栏杆无法去除。为此先使用背景减法的方法，用图 5c 减去前景深度图 5a，去掉限位栏杆等静态背景的深度数据，得到图 6a。猪体高度一般位于 30 ~ 70 cm 之间，对图 6a 二值化得到二值图像，猪体轮廓已经较完整地提取出来，但还有部分粒子需要进行填充和过滤以去除干扰，最终猪体轮廓如图 6b 所示。

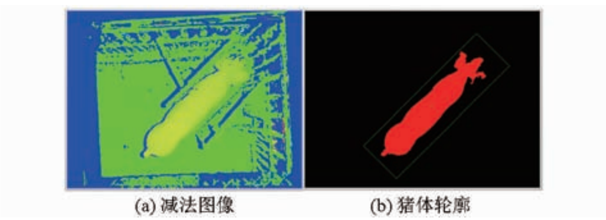

图 6　深度减法图像二值化

Fig. 6　Binarization of depth subtraction image

1.2.4　体尺检测算法

本实验室提出的基于凸包分析的猪体头部与尾部去除算法可以检测猪尾根和耳根分割点[2,23]，体尺检测关键点计算步骤如下：

（1）计算猪体粒子的包络线，计算包络线和轮廓重合点。

（2）计算相邻重合点之间包络线段的长度，筛选出长度大于 30 像素的包络线段。

（3）计算轮廓线段上所有点到包络线段的距离 d_n，选出距离最大的点作为尾根和耳根分割点的备选点，最大距离称为凹陷的深度，如图 7 所示。

图 7　凹陷结构示意图

Fig. 7　Diagram of concave structure

（4）由于饮水器的位置固定，所以猪头的朝向可以确定，以猪体粒子短轴（S）作为分割线，将备选点分为耳根备选点和尾根备选点；距离短轴最远的 2 个尾根备选点为尾根分割点，距离短轴最近的 2 个耳根备选点为脖颈分割点。

上述算法第 2 步使用了像素参数，当系统的物距或相机参数发生变化时，固定像素筛选条件就容易失效。本系统的相机分辨率较高，图 8 的包络线段长度如图 9 所示，看出仅有少数耳根和尾根分割点对应的包络线段较长，若选择长度大于 30 像素的包络线段，将造成线段数量过多，给后续的筛选造成困难；若相机像素数较少或物距较大，包络线段长度会缩短，30 像素的筛选条件可能会造成漏选。由图 8 看出，猪体轮廓较为明显的角点有：尾部 2 个、腹部和臀部连接处 2 个、腹部和肩部连接处 2 个、颈部 2 个以及头部和耳朵的连接处 2 个，共计 10 个角点，因此本研究使用比例系数筛选，只选择包络线段最长的 10 条。

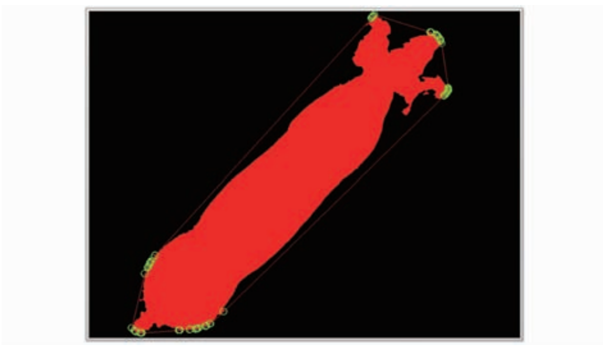

图 8　包络和猪体轮廓重合点

Fig. 8　Coincident points between convex hull and pig contour

算法第 4 步选择耳根和尾根截取点时使用最远和最近的角点，当猪肩部较宽时，包络线会在肩部重合，该方法可能会选择肩部与腹部的角点，造成误选。为解决这个问题，本研究提出一个参数，称为角点的猪体比例归一化系数，即角点到短轴的距离除以猪体粒子长度（l）的一半，如图 10 所示。

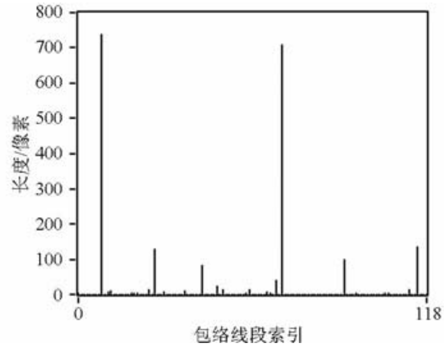

图 9　包络线段长度

Fig. 9　Length of convex hull line segment

图 10　猪体轮廓角点

Fig. 10　Corners of pig body contour

$$R=\frac{2d_n}{l} \tag{8}$$

由于猪尾巴活动范围较小，且多数育肥猪需要剪尾，尾巴长度占身体总长度的比例较小，经过多幅图像测试，猪尾根分割点的系数一般处于 0.43 ~ 0.5 之间；猪体头部活动较大，所以颈部分割点的系数 R 一般处于 0.25 ~ 0.4 之间。

经以上筛选得到猪耳根和尾根分割点如图 11 所示。本研究仅检测便于手工验证的 5 个体尺，体尺测点的提取示意图如图 12 所示。首先确定耳根分割点 1 和 2 的中点 5，以及尾根分割点 3 和 4 的中点 12；点 5 到点 12 为猪只体长；然后从点 1、2 沿猪体粒子长轴方向向后 1/12 ~ 1/3 体长的距离确定矩形 a_1，在矩形 a_1 内寻找猪轮廓最大宽度为肩宽；从点 3、4 向前 1/12 ~ 1/3 体长的距离确定矩形 b_1，在矩形 b_1 内寻找最大宽度为臀宽；2 个体宽测量点的中点为体高测量点；2 个臀宽测量点的中点为臀高测量点。每个体尺计算公式如表 1 所示。

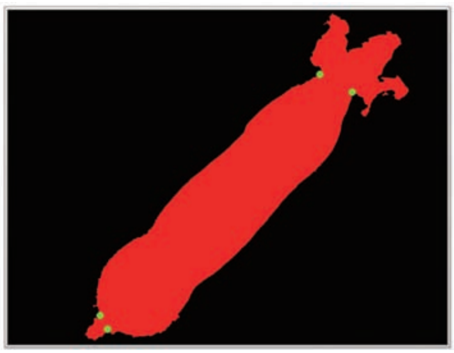

图 11　猪头部和尾部切割点

Fig. 11　Cut points of pig head and tail

图 12　体尺自动检测关键点

Fig. 12　Automatic detection of body measurements key points

1、2. 耳根截取点　3、4. 尾根分割点　5. 颈部中点　6、7. 肩宽测量点　8. 体高测量点　9、10. 臀宽测量点　11. 臀高测量点　12. 尾根中点

表 1　计算体尺公式

Tab. 1　Equation of body size measurement

体尺	计算点序号	描述	公式
体长	5,12	水平距离	$\sqrt{(x_5-x_{12})^2+(y_5-y_{12})^2}$
体宽	6,7	水平距离	$\sqrt{(x_6-x_7)^2+(y_6-y_7)^2}$
体高	8,B8 *	垂直距离	$z_{B8}-z_8$
臀宽	9,10	水平距离	$\sqrt{(x_9-x_{10})^2+(y_9-y_{10})^2}$
臀高	11,B11	垂直距离	$z_{B11}-z_{11}$

* B 代表背景图像上的点。

1.3　系统精度验证

1.3.1　系统检测精度验证

为验证系统检测精度，在实验室使用标定板开展不同距离和不同区域 X、Y、Z 轴检测精度验证。检测标准物体为 10 × 7 的圆点矩阵标定板，圆心间距为 4 cm。检测对象为圆点圆心 X、Y 轴的间距和 Z 轴的高度。相机距离地面高度约为 192 cm。

分别采集 15 个不同高度的标定板图像，高度范围为 0 ~ 80 cm，手工测量标定板 4 个边缘的高度，取平均值；拍摄 3 对左右图像，计算深度图像和圆点圆心的 X、Y、Z 坐标，及圆点圆心的 X 轴、Y 轴间距。Z 轴距离与地面深度相减，获得标定板圆心与地面的距离，对所有距离取均值。

将整个场景划分为左上、左下、右上、右下和中部 5 个区域，在各个区域分别采集距离相机 150 cm 处的标定板图像，计算内容同上，每个区域取 3 张图像的均值。

1.3.2　猪体尺测量精度验证

在天津市惠康种猪育种有限公司 9 号育肥舍，选取 6 号猪圈的 16 头长白育肥猪，猪日龄为 141 ~ 149 d。在 2014 年 6 月 25 日和 7 月 2 日，分别测量

猪的体尺数据。使用卷尺测量猪的体长、体宽、体高、臀宽、臀高,精度为0.1 cm。由于猪只在称重笼中将处于应激状态,为保证测量数据的准确性,应在自由状态下测量猪体尺,尽量选择猪饮水或采食时,猪体处于稳定平直时测量,避免不同姿势影响猪体尺数据[24],每个体尺测量3次取均值。其中每个体尺的测量位置如表2所示。

表2　体尺测量关键点

Tab. 2　Key points of body measurement

体尺	起始点
体长	耳根中点至尾根中点
体宽	肩胛骨最宽两点
体高	肩胛骨最宽处高度
臀宽	臀部最宽两点
臀高	臀部最宽处高度

从每头猪当天的图像中,手工选取深度图像质量较好的,猪体平直无弯曲的图像,使用体尺自动测量程序检测5个体尺,体尺取3张图像测量的平均值。

2　系统验证与结果分析

2.1　标定板检测精度结果

不同距离的 X、Y、Z 轴检测精度如图13所示。Z 轴相对误差随着物距的减小而减小,基本符合检测精度计算公式(6)中检测精度和物距的关系,其中 X 轴、Y 轴检测平均相对误差皆为0.65%,最大相对误差为距离157 cm的0.84%,最小相对误差为120 cm的0.52%;Z 轴检测平均相对误差为0.34%,最小相对误差为136 cm的0.09%,最大相对误差为146 cm的0.72%。系统整体达到较高的检测精度,X、Y 轴检测误差较接近,Z 轴误差普遍小于 X、Y 轴。

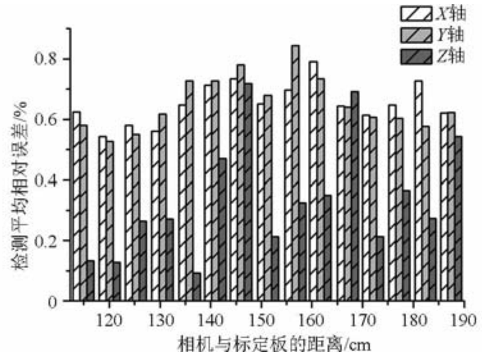

图13　不同高度检测精度

Fig. 13　Detection precision at different heights

不同区域检测精度如图14所示,可见相机视野中央检测精度较高,这也符合镜头畸变的影响规律。故安装相机时,应将猪放在视野中央的位置,并且减少相机与猪体的距离,以提高系统检测精度。

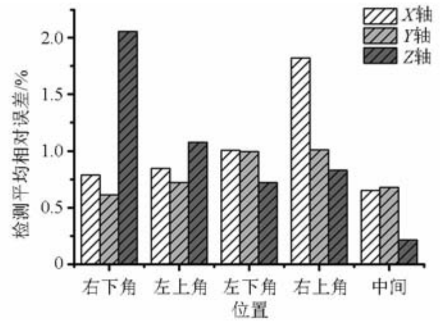

图14　不同区域检测精度

Fig. 14　Detection precision at different area

2.2　猪体尺测量精度结果

对2014年6月25日和7月2日的32组体尺图像检测误差如图15所示,所有体尺的平均绝对误差小于1.5 cm,多数体尺误差小于3 cm,只有部分体长和体高、臀高误差较大。如表3所示,5个体尺的检测平均误差均小于2 cm,体宽、臀宽的检测误差小于1 cm,但由于宽度数量级较小,体宽和臀宽的相对误差分别为3.05%和2.25%。

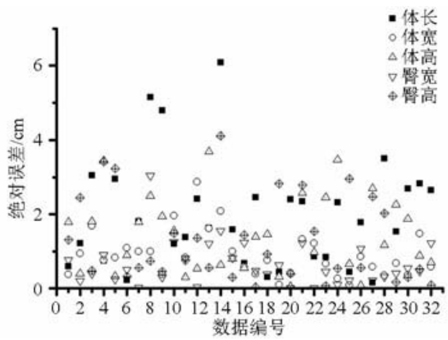

图15　体尺检测绝对误差

Fig. 15　Error of body size detection

表3　体尺检测平均误差

Tab. 3　Average error of body size detection

体尺	绝对误差/cm	相对误差/%
体长	1.97 ± 1.45	1.89 ± 1.37
体宽	0.91 ± 0.62	3.05 ± 2.11
体高	1.43 ± 1.03	2.58 ± 1.92
臀宽	0.66 ± 0.61	2.25 ± 2.04
臀高	1.28 ± 1.15	2.09 ± 1.92

2.3　讨论

由表3可看出,体宽的绝对误差高于臀宽,体高的绝对误差高于臀高,这主要是由于猪的头部较臀部活动较大,容易影响体宽、体高的测量,在本研究中,虽然挑选猪体较平直的图像,但由于猪在饮水时喜欢玩耍饮水器,姿势经常变化,造成体宽和体高测量值误差较大。建议通过1 d内采集的大量图像,获取较为准确的体尺数据。

另外由于猪天性好动,很难保证抓拍照片或测

量体尺时，能够保持静止和标准的姿势，而且养殖户并不需要时刻检测猪体尺，每天 1 次的检测频率可满足要求，为减小体质量估测误差，应对估测的图像严格筛选，开发自动筛选程序，并剔除粗大误差，如此可以获得较准确的体尺。

3　结论

（1）提出基于深度图像的背景减法提取猪体轮廓的方法，经猪场试验测试，对光照和猪体背部脏污不敏感。

（2）改进基于凹陷分析的体尺关键点检测算法，使用相对比例替代像素参数筛选包络线段，使用角点的猪体比例归一化系数筛选头部和尾部分割点，提高系统的实用性和稳定性。

（3）实验室试验表明，2 m 的物距范围内，系统的三维检测相对误差在 1% 以内。现场试验对 16 头猪 32 组体尺检测平均相对误差在 2% 左右，所有体尺的检测平均误差小于 2 cm，系统可以准确检测猪只体尺。

参　考　文　献

1　DOESCHL-WILSON A B, GREEN D M, FISHER A V, et al. The relationship between body dimensions of living pigs and their carcass composition[J]. Meat Science, 2005, 70(2): 229 – 240.

2　付为森. 基于双目视觉的猪体尺检测与体重预估方法研究[D]. 北京：中国农业大学, 2011.
FU Weisen. Study of pig's body dimensions detection and weight estimation based-on binocular stereovision [D]. Beijing: China Agricultural University, 2011. (in Chinese)

3　杨艳. 基于计算机视觉技术的种猪体尺和体重估算方法研究[D]. 北京：中国农业大学, 2006.
YANG Yan. Study on the estimation of pig's dimensions and weight based on computer vision techniques[D]. Beijing: China Agricultural University, 2006. (in Chinese)

4　郭浩. 动物体表三维数据获取与处理算法研究[D]. 北京：中国农业大学, 2015.
GUO Hao. Study on 3D data capturing and processing methods for live animal[D]. Beijing: China Agricultural University, 2015. (in Chinese)

5　郭浩，马钦，张胜利，等. 基于三维重建的动物体尺获取原型系统[J]. 农业机械学报, 2014, 45(5): 227 – 232.
GUO Hao, MA Qin, ZHANG Shengli, et al. Prototype system of shape measurements of animal based on 3D reconstruction[J]. Transactions of the Chinese Society for Agricultural Machinery, 2014, 45(5): 227 – 232. (in Chinese)

6　TASDEMIR Sakir, URKMEZ Abdullah, INAL Seref. Determination of body measurements on the Holstein cows using digital image analysis and estimation of live weight with regression analysis[J]. Computers and Electronics in Agriculture, 2011, 76(2): 189 – 197.

7　TASDEMIR Sakir, URKMEZ Abdullah, Inal Seref. A fuzzy rule-based system for predicting the live weight of Holstein cows whose body dimensions were determined by image analysis[J]. Turkish Journal of Electrical Engineering and Computer Sciences, 2011, 19(4): 689 – 703.

8　OCHOA Zaragoza Luis Enrique. Evaluation of the accuracy of simple body measurements for live weight prediction in growing-finishing pigs[D]. Champaign: University of Illinois at Urbana-Champaign, 2010.

9　ENEVOLDSEN Carsten, KRISTENSEN Troels. Estimation of body weight from body size measurements and body condition scores in dairy cows[J]. Journal of Dairy Science, 1997, 80(9): 1988 – 1995.

10　BRANDL Nabil, JØRGENSEN Erik. Determination of live weight of pigs from dimensions measured using image analysis[J]. Computers and Electronics in Agriculture, 1996, 15(1): 57 – 72.

11　杨艳，滕光辉，李保明，等. 基于计算机视觉技术估算种猪体重的应用研究[J]. 农业工程学报, 2006, 22(2): 127 – 131.
YANG Yan, TENG Guanghui, LI Baoming, et al. Measurement of pig weight based on computer vision[J]. Transactions of the CSAE, 2006, 22(2): 127 – 131. (in Chinese)

12　付为森，滕光辉，杨艳. 种猪体重三维预估模型的研究[J]. 农业工程学报, 2006, 22(14): 84 – 87.
FU Weisen, TENG Guanghui, YANG Yan. Research on three-dimensional model of pig's weight estimating[J]. Transactions of the CSAE, 2006, 22(14): 84 – 87. (in Chinese)

13　VIAZZI S, BAHR C, VAN HERTEM T, et al. Comparison of a three-dimensional and two-dimensional camera system for automated measurement of back posture in dairy cows[J]. Computers and Electronics in Agriculture, 2014, 100(1): 139 – 147.

14　MENESATTI Paolo, COSTA Corrado, ANTONUCCI Francesca, et al. A low-cost stereovision system to estimate size and weight of live sheep[J]. Computers and Electronics in Agriculture, 2014, 103(4): 33 – 38.

15　吴鑫，王桂英，丛杨. 基于颜色和深度信息融合的目标识别方法[J]. 农业工程学报, 2013, 29(25): 96 – 100.
WU Xin, WANG Guiying, CONG Yang. Object recognition method by combining color and depth information[J]. Transactions of the CSAE, 2013, 29(25): 96 – 100. (in Chinese)

16　KONGSRO Jørgen. Estimation of pig weight using a Microsoft Kinect prototype imaging system[J]. Computers and Electronics in Agriculture, 2014, 109(11): 32 – 35.

17　郭浩，王鹏，马钦，等. 基于深度图像的奶牛体型评定指标获取技术[J]. 农业机械学报, 2013, 44(增刊 1): 273 – 276.

GUO Hao, WANG Peng, MA Qin, et al. Acquisition of appraisal traits for dairy cow based on depth image[J]. Transactions of the Chinese Society for Agricultural Machinery, 2013, 44(Supp.1): 273 - 276. (in Chinese)

18 刘波,朱伟兴,杨建军,等. 基于深度图像和生猪骨架端点分析的生猪步频特征提取[J]. 农业工程学报, 2014, 30(10): 131 - 137.

LIU Bo, ZHU Weixing, YANG Jianjun, et al. Extracting of pig gait frequency feature based on depth image and pig skeleton endpoints analysis[J]. Transactions of the CSAE, 2014, 30(10): 131 - 137. (in Chinese)

19 李卓,毛涛涛,刘同海,等. 基于机器视觉的猪体质量估测模型比较与优化[J]. 农业工程学报, 2015, 21(2): 155 - 161.

LI Zhuo, MAO Taotao, LIU Tonghai, et al. Comparison and optimization of pig mass estimation models based on machine vision [J]. Transactions of the CSAE, 2015, 21(2): 155 - 161. (in Chinese)

20 BRADSKI G, KAEHLER A. Learning OpenCV: computer vision with the OpenCV library[M]. Sebastopol, CA: O'Reilly Media Inc, 2008: 442.

21 刘昭华,杨玉霞,马大喜,等. 半全局匹配算法的多基线扩展及 GPU 并行处理方法[J]. 测绘科学, 2014, 39(11): 99 - 103.

LIU Zhaohua, YANG Yuxia, MA Daxi, et al. Study on semi-global matching algorithm extended for multi baseline matching and parallel processing method based on GPU[J]. Science of Surveying and Mapping, 2014, 39(11): 99 - 103. (in Chinese)

22 HIRSCHMULLER Heiko. Stereo processing by semiglobal matching and mutual information[J]. IEEE Transactions on Pattern Analysis and Machine Intelligence, 2008, 30(2): 328 - 341.

23 刘同海,滕光辉,付为森,等. 基于机器视觉的猪体体尺测点提取算法与应用[J]. 农业工程学报, 2013, 29(2): 161 - 168.

LIU Tonghai, TENG Guanghui, FU Weisen, et al. Extraction algorithms and applications of pig body size measurement points based on computer vision[J]. Transactions of the CASE, 2013, 29(2): 161 - 168. (in Chinese)

24 LI Zhuo, LUO Cheng, TENG Guanghui, et al. Estimation of pig weight by machine vision: a review[C]// Computer and Computing Technologies in Agriculture, 2013,2:42 - 49.

(上接第 297 页)

19 LI F, MIAO Y, FENG G, et al. Improving estimation of summer maize nitrogen status with red edge-based spectral vegetation indices[J]. Field Crops Research, 2014, 157(2): 111 - 123.

20 陈兵,韩焕勇,王方永,等. 利用光谱红边参数监测黄萎病棉叶叶绿素和氮素含量[J]. 作物学报,2013,39(2):319 - 329.

CHEN Bing, HAN Huanyong, WANG Fangyong, et al. Monitoring chlorophyll and nitrogen contents in cotton leaf infected by verticillium wilt with spectra red edge parameters [J]. Actc Agronomica Sinica, 2013, 39(2): 319 - 329. (in Chinese)

21 蒋金豹,陈云浩,黄文江. 利用高光谱红边与黄边位置距离识别小麦条锈病[J]. 光谱学与光谱分析,2010,30(6):1614 - 1618.

JIANG Jinbao, CHEN Yunhao, HUANG Wenjiang. Using the distance between hyperspectral red edge position and yellow edge position to identify wheat yellow rust disease [J]. Spectroscopy and Spectral Analysis, 2010, 30(6): 1614 - 1618. (in Chinese)

22 冯伟,朱艳,姚霞,等. 利用红边特征参数监测小麦叶片氮素积累状况[J]. 农业工程学报,2009,25(11):194 - 201.

FENG Wei, ZHU Yan, YAO Xia, et al. Monitoring nitrogen accumulation in wheat leaf with red edge characteristics parameters [J]. Transactions of the CSAE, 2009,25(11): 194 - 201. (in Chinese)

23 ZHANG Jinheng, WANG Ke. New vegetation index for estimating nitrogen concentration using fresh leaf spectral reflectance [J]. Transactions of the CSAE, 2008, 24(3): 158 - 161.

24 JU Changhua, TIAN Yongchao, YAO Xia, et al. Estimating leaf chlorophyll content using red edge parameters[J]. Pedosphere, 2010, 20(5): 633 - 644.

25 张永贺,郭啸川,褚武道,等. 基于红边位置的木荷叶片叶绿素含量估测模型研究[J]. 红外与激光工程,2013, 42(3): 798 - 804.

ZHANG Yonghe, GUO Xiaochuan, CHU Wudao, et al. Estimation model of schima superba leaf chlorophyll content based on red edge position [J]. Infrared and Laser Engineering, 2013, 42(3): 798 - 804. (in Chinese)

26 CHO M A, SKIDMORE A K. A new technique for extracting the red edge position from hyperspectral data: the linear extrapolation method [J]. Remote Sensing of Environment, 2006, 101(2): 181 - 193.

27 薛利红, 杨林章. 采用不同红边位置提取技术估测蔬菜叶绿素含量的比较研究[J]. 农业工程学报,2008, 24(9): 165 - 169.

XUE Lihong, YANG Linzhang. Comparative study on estimation of chlorophyll content in spinach leaves using various red edge position extraction techniques [J]. Transactions of the CSAE, 2008,24(9): 165 - 169. (in Chinese)